

# Making Offline RL Online: Collaborative World Models for Offline Visual Reinforcement Learning

Qi Wang<sup>\*12</sup> Junming Yang<sup>\*3</sup> Yunbo Wang<sup>1</sup> Xin Jin<sup>2</sup> Wenjun Zeng<sup>2</sup> Xiaokang Yang<sup>1</sup>

## Abstract

Training offline reinforcement learning (RL) models using visual inputs poses two significant challenges, *i.e.*, the overfitting problem in representation learning and the overestimation bias for expected future rewards. Recent work has attempted to alleviate the overestimation bias by encouraging conservative behaviors. This paper, in contrast, tries to build more flexible constraints for value estimation without impeding the exploration of potential advantages. The key idea is to leverage off-the-shelf RL simulators, which can be easily interacted with in an online manner, as the “test bed” for offline policies. To enable effective online-to-offline knowledge transfer, we introduce CoWorld, a model-based RL approach that mitigates cross-domain discrepancies in state and reward spaces. Experimental results demonstrate the effectiveness of CoWorld, outperforming existing RL approaches by large margins.

## 1. Introduction

Learning control policies with visual observations can be challenging due to high interaction costs with the physical world. Offline reinforcement learning (RL) is a promising approach to address this challenge (Fujimoto et al., 2019; Kumar et al., 2020; Qi et al., 2022; Chen et al., 2023; Zhuang et al., 2023). However, the direct use of current offline RL algorithms in visual control tasks presents two primary difficulties. Initially, *offline visual RL* is more prone to overfitting issues during representation learning, as it involves extracting hidden states from the limited, high-dimensional visual inputs. Moreover, like its state-space counterpart, offline visual RL is susceptible to the challenge of value overestimation, as we observe from existing methods (Laskin

<sup>\*</sup>Equal contribution <sup>1</sup>MoE Key Lab of Artificial Intelligence, AI Institute, Shanghai Jiao Tong University, Shanghai, China <sup>2</sup>Eastern Institute for Advanced Study, Zhengjiang, China <sup>3</sup>Nanjing University of Posts and Telecommunications, Nanjing, China. Correspondence to: Yunbo Wang <yunbow@sjtu.edu.cn>.

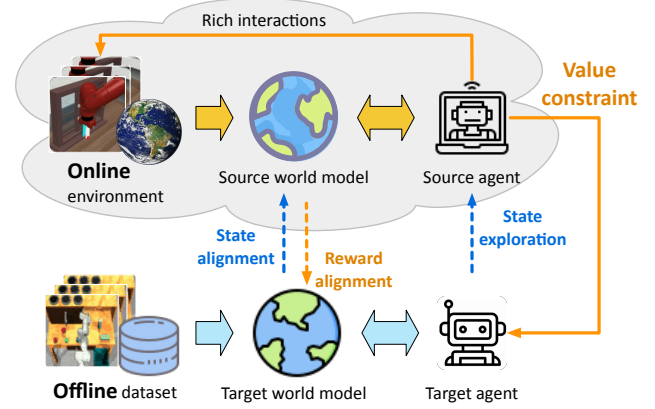


Figure 1. Our approach solves offline visual RL through a transfer learning paradigm. It harnesses cross-domain knowledge to provide flexible constraints for value estimation on the offline dataset, without impeding state exploration with potential advantages.

et al., 2020; Hafner et al., 2021).

Improving offline visual RL remains an under-explored research area. Our goal is to strike a balance between value overestimation and over-conservatism (when excessively penalizing the estimated values beyond the offline data distribution). Intuitively, **we should not overly constrain the state exploration with potential advantages**. Our basic idea, as illustrated in Figure 1, is to leverage readily available online simulators for related (not necessarily identical) visual control tasks as auxiliary source domains, so that we can frame offline visual RL as an *offline-online-offline* transfer learning problem to learn mildly conservative policies.

We present a novel model-based transfer RL approach called Collaborative World Models (CoWorld). Specifically, we train separate world models and RL agents for source and target domains, each with domain-specific parameters. To mitigate discrepancies between the world models, we introduce a novel representation learning scheme comprising two iterative training stages. These stages, as shown in Figure 1, facilitate the alignment of latent state distributions (*offline to online*) and reward functions (*online to offline*), respectively. By doing so, the source domain critic can serve as an online “test bed” for assessing the target offline policy. It is also more “knowledgeable” as it can actively interact with the online environment and gather rich information.

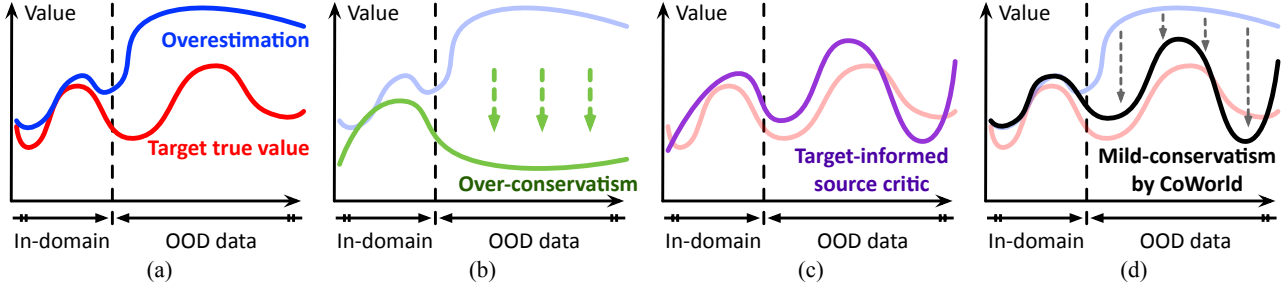


Figure 2. To address value overestimation in offline RL (a), we can directly penalize the estimated values beyond the distribution of offline data, which may hinder the agent’s exploration of potential states with high rewards (b). Unlike existing methods, CoWorld trains a cross-domain critic model in an online auxiliary domain to reassess the offline policy (c), and regularizes the target values with flexible constraints (d). The feasibility of this approach lies in the domain alignment techniques during the world model learning stage.

Table 1. Similarities and discrepancies between RoboDesk (*target domain*) and Meta-World (*auxiliary source domain*) environments.

	Source: <i>Meta-World</i>	Target: <i>RoboDesk</i>	Similarity / Difference
Task	Window Close	Open Slide	Related manipulation tasks
Dynamics	Simulated Sawyer robot arm	Simulated Franka Emika Panda robot arm	Different
Action space	Box(-1, 1, (4,), float64)	Box(-1, 1, (5,), float32)	Different
Reward scale	[0, 1]	[0, 10]	Different
Observation	Right-view images	Top-view images	Different view points

Another benefit of the domain-collaborative world models is the ability to alleviate overfitting issues associated with offline representation learning, leading to more generalizable latent states derived from limited offline visual data.

For behavior learning in the offline dataset, we exploit the knowledge from the source model and introduce a mild regularization term to the training objective of the target domain critic model. This regularization term encourages the **source critic** to reevaluate the **target policy**. As illustrated in Figure 2, it allows for flexible constraint on overestimated values of trajectories that receive low values from the “knowledgeable” source critic. Conversely, if a policy yields high values from the source critic, we prefer to retain the original estimation by the offline agent. This approach is feasible because the source critic has been aligned with the target domain during world model learning.

We showcase the effectiveness CoWorld in offline visual control tasks across the Meta-World, RoboDesk, and DeepMind Control benchmarks. Our approach is shown to be readily extendable to scenarios with multiple source domains. It effectively addresses value overestimation by transferring knowledge from auxiliary domains, even in the presence of diverse physical dynamics, action spaces, reward scales, and visual appearances.

In summary, our work brings the following contributions:

- We innovatively frame offline visual RL as a domain transfer problem. The fundamental idea is to harness cross-domain knowledge to tackle representation overfitting and value overestimation in offline visual control tasks.
- We present CoWorld, a method that follows the offline-

online-offline paradigm, incorporating specific techniques of world model alignment and flexible value constraints.

## 2. Problem Setup

We consider offline visual reinforcement learning as a partially observable Markov decision process (POMDP) that aims to maximize the cumulative reward in a fixed target dataset  $\mathcal{B}^{(T)}$ . We specifically focus on scenarios where auxiliary environments are accessible, enabling rich interactions and efficient online data collection. The goal is to improve the offline performance of the target POMDP  $\langle \mathcal{O}^{(T)}, \mathcal{A}^{(T)}, \mathcal{T}^{(T)}, \mathcal{R}^{(T)}, \gamma^{(T)} \rangle$  through knowledge transfer from the source POMDPs  $\langle \mathcal{O}^{(S)}, \mathcal{A}^{(S)}, \mathcal{T}^{(S)}, \mathcal{R}^{(S)}, \gamma^{(S)} \rangle$ . These notations respectively denote the space of visual observations, the space of actions, the state transition probabilities, the reward function, and the discount factor.

For example, in one of our experiments, we employ RoboDesk as the offline target domain and various tasks from Meta-World as the source domains. As illustrated in Table 1, these two environments present notable distinctions in physical dynamics, action spaces, reward definitions, and visual appearances as the observed images are from different camera views. Our priority is to address domain discrepancies to enable cross-domain behavior learning.

## 3. Method

In this section, we present the technical details of CoWorld, which consists of a pair of world models  $\{\mathcal{M}_{\phi'}, \mathcal{M}_{\phi}\}$ , actor networks  $\{\pi_{\psi'}, \pi_{\psi}\}$ , and critic networks  $\{v_{\xi'}, v_{\xi}\}$ , where

$\{\phi, \psi, \xi\}$  and  $\{\phi', \psi', \xi'\}$  are respectively target and source domain parameters. As potential cross-domain discrepancies may exist in all elements of  $\{\mathcal{O}, \mathcal{A}, \mathcal{T}, \mathcal{R}\}$ , the entire training process is organized into three iterative stages, following an *offline-online-offline* transfer learning framework:

- A) *Offline-to-online state alignment*: Train  $\mathcal{M}_\phi$  by aligning its state space with that of the source  $\mathcal{M}_{\phi'}$ .
- B) *Online-to-offline reward alignment*: Train  $\mathcal{M}_{\phi'}$  and  $\{\pi_{\psi'}, v_{\xi'}\}$  in the online environment by incorporating the target reward information.
- C) *Online-to-offline value constraint*: Train  $\{\pi_{\psi'}, v_{\xi'}\}$  with value constraints provided by the source critic  $v_{\xi'}$ .

### 3.1. Offline-to-Online State Alignment

**Source model pretraining.** We start with a source domain warm-up phase employing a model-based actor-critic method known as DreamerV2 (Hafner et al., 2021). To facilitate cross-domain knowledge transfer, we additionally introduce a state alignment module, which is denoted as  $g(\cdot)$  and implemented using the softmax operation. The world model  $\mathcal{M}_{\phi'}$  consists of the following components:

$$\begin{aligned}
 \text{Recurrent transition:} \quad & h_t^{(S)} = f_{\phi'}(h_{t-1}^{(S)}, z_{t-1}^{(S)}, a_{t-1}^{(S)}) \\
 \text{Image encoding:} \quad & e_t^{(S)} = e_{\phi'}(o_t^{(S)}) \\
 \text{Posterior state:} \quad & z_t^{(S)} \sim q_{\phi'}(h_t^{(S)}, e_t^{(S)}) \\
 \text{Prior state:} \quad & \hat{z}_t^{(S)} \sim p_{\phi'}(h_t^{(S)}) \\
 \text{Reconstruction:} \quad & \hat{o}_t^{(S)} \sim p_{\phi'}(h_t^{(S)}, z_t^{(S)}) \\
 \text{Reward prediction:} \quad & \hat{r}_t^{(S)} \sim r_{\phi'}(h_t^{(S)}, z_t^{(S)}) \\
 \text{Discount factor:} \quad & \hat{\gamma}_t^{(S)} \sim p_{\phi'}(h_t^{(S)}, z_t^{(S)}) \\
 \text{State alignment target:} \quad & s_t^{(S)} = g(e_t^{(S)}),
 \end{aligned} \tag{1}$$

where  $\phi'$  represents the combined parameters of the world model. We train  $\mathcal{M}_{\phi'}$  on the dynamically expanded source domain experience replay buffer  $\mathcal{B}^{(S)}$  by minimizing

$$\begin{aligned}
 \mathcal{L}(\phi') = \mathbb{E}_{q_{\phi'}} \left[ \sum_{t=1}^T \underbrace{-\ln p_{\phi'}(o_t^{(S)} | h_t^{(S)}, z_t^{(S)})}_{\text{image reconstruction}} \right. \\
 \underbrace{-\ln r_{\phi'}(r_t^{(S)} | h_t^{(S)}, z_t^{(S)})}_{\text{reward prediction}} - \underbrace{\ln p_{\phi'}(\gamma_t^{(S)} | h_t^{(S)}, z_t^{(S)})}_{\text{discount prediction}} \\
 \left. + \underbrace{\text{KL} [q_{\phi'}(z_t^{(S)} | h_t^{(S)}, o_t^{(S)}) \parallel p_{\phi'}(\hat{z}_t^{(S)} | h_t^{(S)})]}_{\text{KL divergence}} \right]. \tag{2}
 \end{aligned}$$

We train the source actor  $\pi_{\psi'}(\hat{z}_t)$  and critic  $v_{\xi'}(\hat{z}_t)$  with the respective objectives of maximizing and estimating the expected future rewards  $\mathbb{E}_{p_{\phi'}, p_{\psi'}} [\sum_{\tau \geq t} \hat{\gamma}_{\tau-t} \hat{r}_{\tau}]$  generated by  $\mathcal{M}_{\phi'}$ . Please refer to Appendix A.3 for more details. We deploy  $\pi_{\psi'}$  to interact with the auxiliary environment and collect new data for further world model training.

**State alignment.** A straightforward transfer learning solution is to train the target agent in the offline dataset upon the checkpoints of the source agent. However, it may suffer from a potential mismatch issue due to the discrepancy in tasks, visual observations, physical dynamics, and action spaces across various domains. This becomes more severe when the online data is collected from environments that differ from the offline dataset (e.g., Meta-World  $\rightarrow$  RoboDesk). We tackle this issue by separating the parameters of the source and the target agents while explicitly aligning their latent state spaces. Concretely, the target world model  $\mathcal{M}_\phi$  has an identical network architecture to the source model  $\mathcal{M}_{\phi'}$ . We feed the same target domain observations sampled from  $\mathcal{B}^{(T)}$  into these models and close the distance of  $e_{\phi'}(o_t^{(T)})$  and  $e_\phi(o_t^{(T)})$ . We optimize  $\mathcal{M}_\phi$  by minimizing

$$\begin{aligned}
 \mathcal{L}(\phi) = \mathbb{E}_{q_\phi} \left[ \sum_{t=1}^T \underbrace{-\ln p_\phi(o_t^{(T)} | h_t^{(T)}, z_t^{(T)})}_{\text{image reconstruction}} \right. \\
 \underbrace{-\ln r_\phi(r_t^{(T)} | h_t^{(T)}, z_t^{(T)})}_{\text{reward prediction}} - \underbrace{\ln p_\phi(\gamma_t^{(T)} | h_t^{(T)}, z_t^{(T)})}_{\text{discount prediction}} \\
 + \underbrace{\beta_1 \text{KL} [q_\phi(z_t^{(T)} | h_t^{(T)}, o_t^{(T)}) \parallel p_\phi(\hat{z}_t^{(T)} | h_t^{(T)})]}_{\text{KL divergence}} \\
 \left. + \underbrace{\beta_2 \text{KL} [\text{sg}(g(e_{\phi'}(o_t^{(T)}))) \parallel g(e_\phi(o_t^{(T)}))]}_{\text{domain alignment loss}} \right], \tag{3}
 \end{aligned}$$

where  $\text{sg}(\cdot)$  indicates gradient stopping and we use the encoding from the source model as the state alignment target. As the source world model can actively interact with the online environment and gather rich information, it keeps the target world model from overfitting the offline data. The importance of this loss term is governed by  $\beta_2$ . We examine its sensitivity in the experiments.

### 3.2. Online-to-Offline Reward Alignment

To enable the source agent to value the target policy, it is essential to provide it with prior knowledge of the offline task. To achieve this, we train the source reward predictor  $r_{\phi'}(\cdot)$  using mixed data from both of the replay buffers  $\mathcal{B}^{(S)}$  and  $\mathcal{B}^{(T)}$ . Through the behavior learning on source domain imaginations, the target-informed reward predictor enables the source RL agent to assess the imagined states produced by the target model and provide a flexible constraint to target value estimation (as we will discuss in Section 3.3).

Specifically, we first sample a target domain data trajectory  $\{(o_t^{(T)}, a_t^{(T)}, r_t^{(T)})\}_{t=1}^T$  from  $\mathcal{B}^{(T)}$  (Line 19 in Alg. 1). We then use the source world model parametrized by  $\phi'$  to extract corresponding latent states and relabel the *target-informed source reward* (Line 20 in Alg. 1):

**Algorithm 1** The training scheme of CoWorld.

---

```

1: Require: Offline dataset  $\mathcal{B}^{(T)}$ .
2: Initialize: Parameters of the source model  $\{\phi', \psi', \xi'\}$  and
   the target model  $\{\phi, \psi, \xi\}$ .
3: Pretrain the source agent and collect a replay buffer  $\mathcal{B}^{(S)}$ .
4: while not converged do
5:   // In the offline domain:
6:   for each step in  $\{1 : K_1\}$  do
7:     Sample  $\{(o_t^{(T)}, a_t^{(T)}, r_t^{(T)})\}_{t=1}^T \sim \mathcal{B}^{(T)}$ .
8:     // Offline-to-online state alignment
9:     Train the target world model  $\mathcal{M}_\phi$  using Eq. (3).
10:    // Behavior learning with constraint
11:    Generate  $\{(z_i^{(T)}, a_i^{(T)})\}_{i=t}^{t+H}$  using  $\pi_\psi$  and  $\mathcal{M}_\phi$ .
12:    Train the critic  $v_\xi$  using Eq. (6) over  $\{(z_i^{(T)}, a_i^{(T)})\}_{i=t}^{t+H}$ .
13:    Train the actor  $\pi_\psi$  using Eq. (7) over  $\{(z_i^{(T)}, a_i^{(T)})\}_{i=t}^{t+H}$ .
14:  end for
15:  // In the online domain:
16:  for each step in  $\{1 : K_2\}$  do
17:    Sample  $\{(o_t^{(S)}, a_t^{(S)}, r_t^{(S)})\}_{t=1}^T \sim \mathcal{B}^{(S)}$ .
18:    // Online-to-offline reward alignment
19:    Sample  $\{(o_t^{(T)}, a_t^{(T)}, r_t^{(T)})\}_{t=1}^T \sim \mathcal{B}^{(T)}$ .
20:    Relabel the source rewards  $\{\tilde{r}_t^{(S)}\}_{t=1}^T$  using Eq. (4).
21:    Train  $\mathcal{M}_{\phi'}$  using Eq. (2) combined with Eq. (5).
22:    // Source domain behavior learning
23:    Generate  $\{(z_i^{(S)}, a_i^{(S)})\}_{i=t}^{t+H}$  using  $\pi_{\psi'}$  and  $\mathcal{M}_{\phi'}$ .
24:    Train  $\pi_{\psi'}$  and  $v_{\xi'}$  over the imagined  $\{(z_i^{(S)}, a_i^{(S)})\}_{i=t}^{t+H}$ .
25:    Use  $\pi_{\psi'}$  to collect new source data and append  $\mathcal{B}^{(S)}$ .
26:  end for
27: end while
    
```

---

$$\begin{aligned}
 \tilde{h}_t &= f_{\phi'}(\tilde{h}_{t-1}, \tilde{z}_{t-1}, a_{t-1}^{(T)}) \\
 \tilde{e}_t &= e_{\phi'}(o_t^{(T)}) \\
 \tilde{z}_t &\sim q_{\phi'}(\tilde{h}_t, \tilde{e}_t) \\
 \tilde{r}_t^{(S)} &= (1 - k) \cdot r_{\phi'}(\tilde{h}_t, \tilde{z}_t) + k \cdot r_t^{(T)},
 \end{aligned} \tag{4}$$

where  $k$  is the target-informed reward factor, which acts as a balance between the true target reward  $r_t^{(T)}$  and the output of the source reward predictor  $r_{\phi'}(\cdot)$  provided with target states. It is crucial to emphasize that using the target data as inputs to compute  $r_{\phi'}(\cdot)$  is feasible due to the alignment of the target state space with the source state space.

We jointly use the relabeled reward  $\tilde{r}_t^{(S)}$  and the original source domain reward  $r_t^{(S)}$  sampled from  $\mathcal{B}^{(S)}$  to train the source reward predictor. This training is achieved by minimizing a maximum likelihood estimation (MLE) loss:

$$\begin{aligned}
 \mathcal{L}_r(\phi') &= \eta \cdot \mathbb{E}_{\mathcal{B}^{(S)}} \left[ \sum_{t=1}^T -\ln r_{\phi'}(r_t^{(S)} | h_t^{(S)}, z_t^{(S)}) \right] \\
 &+ (1 - \eta) \mathbb{E}_{\mathcal{B}^{(T)}} \left[ \sum_{t=1}^T -\ln r_{\phi'}(\tilde{r}_t^{(S)} | h_t^{(T)}, z_t^{(T)}) \right],
 \end{aligned} \tag{5}$$

where the second term measures the negative log-likelihood of observing the relabelled source reward  $\tilde{r}_t^{(S)}$ .  $\eta$  represents a hyperparameter that gradually decreases from 1 to 0.1

throughout this training stage. Intuitively,  $\eta$  controls the progressive adaptation of the well-trained source reward predictor to the target domain with limited target reward supervision. We integrate Eq. (5) into Eq. (2) to train the entire world model  $\mathcal{M}_{\phi'}$  for the source domain agent (**Line 21** in Alg. 1) and subsequently perform model-based behavior learning to enable the source critic to assess the target policy (**Lines 23-25** in Alg. 1).

### 3.3. Min-Max Value Constraint

In the behavior learning phase of the target agent (**Lines 11-13** of Alg. 1), we mitigate value overestimation in the offline dataset by introducing a min-max regularization term to the objective function of the target critic model  $v_\xi$ . Initially, we use the auxiliary source critic  $v_{\xi'}$  to estimate the value function of the imagined target states. Following that, we train  $v_\xi$  by additionally **minimizing the maximum value** among the estimates provided by source and target critics:

$$\begin{aligned}
 \mathcal{L}(\xi) &= \mathbb{E}_{p_\phi, p_\psi} \left[ \sum_{t=1}^{H-1} \underbrace{\frac{1}{2} \left( v_\xi(\hat{z}_t^{(T)}) - \text{sg}(V_t^{(T)}) \right)^2}_{\text{value regression}} \right. \\
 &\quad \left. + \underbrace{\alpha \max \left( v_\xi(\hat{z}_t^{(T)}), \text{sg}(v_{\xi'}(\hat{z}_t^{(T)})) \right)}_{\text{value constraint}} \right],
 \end{aligned} \tag{6}$$

where  $V_t^{(T)}$  incorporates a weighted average of reward information over an  $n$ -step future horizon. The first term in the provided loss function fits cumulative value estimates (whose specific formulation can be located in [Appendix A.3](#)), while the second term regularizes the overestimated values for out-of-distribution data in a mildly conservative way. The hyperparameter  $\alpha$  represents the importance of the value constraint. The  $\text{sg}(\cdot)$  operator indicates that we stop the gradient to keep the source critic from being influenced by the regularization term.

This approach provides flexibly conservative value estimations, finding a balance between mitigating overestimation and avoiding excessive conservatism in the value function. When the target critic overestimates the value function, the source critic is less vulnerable to the value overestimation problem as it is trained with rich interaction data. Thus, it is possible to observe  $v_\xi(\hat{z}_t^{(T)}) > v_{\xi'}(\hat{z}_t^{(T)})$ , and our approach is designed to decrease the output of  $v_\xi$  to the output of  $v_{\xi'}$ . This prevents the target critic from overestimating the true value. Conversely, when the source critic produces greater values in  $v_{\xi'}(\hat{z}_t^{(T)})$ , the min-max regularization term does not contribute to the training of the target critic  $v_\xi$ . This encourages the exploration of potentially advantageous states within the imaginations of the target world model.

In line with DreamerV2 ([Hafner et al., 2021](#)), we train the target actor  $\pi_\psi$  by maximizing a REINFORCE objective function with entropy regularization, allowing the gradients



Table 2. Mean episode returns and standard deviations of 10 episodes over 3 seeds on Meta-World.

MODEL	BP→DC*	DC→BP	BT→WC	BP→HP	WC→DC	HP→BT	AVG.
OFFLINE DV2	2143±579	3142±533	3921±752	278±128	3899±679	3002±346	2730
DRQ + BC	567±19	587±68	623±85	1203±234	134±64	642±99	626
CQL	1984±13	867±330	683±268	988±39	577±121	462±67	927
CURL	1972±11	51±17	281±73	986±47	366±52	189±10	641
LOMPO	2883±183	446±458	2983±569	2230±223	2756±331	1961±287	1712
DV2 FINETUNE	3500±414	2456±661	3467±1031	3702±451	4273±1327	3499±713	3781
DV2 FINETUNE + EWC	1566±723	167±86	978±772	528±334	2048±1034	224±147	918
LOMPO FINETUNE	259±191	95±53	142±70	332±452	3698±1615	224±88	792
CoWORLD (BEST-SOURCE)	<b>3967±312</b>	<b>3623±543</b>	<b>4521±367</b>	<b>4570±677</b>	<b>4845±14</b>	<b>3889±159</b>	<b>4241</b>
CoWORLD (MULTI-SOURCE)	<u>3864±352</u>	<u>3573±541</u>	<u>4507±59</u>	<u>4460±783</u>	<u>4678±137</u>	<u>3626±275</u>	<u>4094</u>

to backpropagate directly through the learned dynamics:

$$\mathcal{L}(\psi) = \mathbb{E}_{p_\phi, p_\psi} \left[ \underbrace{\sum_{t=1}^{H-1} (\beta H[a_t^{(T)} | \hat{z}_t^{(T)}])}_{\text{entropy regularization}} + \underbrace{\rho V_t^{(T)}}_{\text{dynamics backprop}} + \underbrace{(1 - \rho) \ln \pi_\psi(\hat{a}_t^{(T)} | \hat{z}_t^{(T)}) \mathbb{S}\mathbb{G}(V_t^{(T)} - v_\xi(\hat{z}_t^{(T)}))}_{\text{REINFORCE}} \right]. \quad (7)$$

As previously mentioned,  $V_t^{(T)}$  involves a weighted average of reward information over an  $n$ -step future horizon, with detailed formulation provided in Appendix A.3.

Furthermore, it is crucial to note that CoWorld can readily be extended to scenarios with multiple source domains by adaptively selecting a useful task as the auxiliary domain. This extension is easily achieved by measuring the distance of the latent states between the target domain and each source domain. For technical details of the adaptive source domain selection method, please refer to Appendix C.

## 4. Experiments

In this section, we present (i) quantitative comparisons with existing visual RL algorithms; (ii) discussions on the influence of discrepancies between the source and target domains; (iii) ablation studies of each proposed training stage; and (iv) further analyses of value overestimation.

### 4.1. Experimental Setups

**Datasets.** We evaluate CoWorld across three visual control environments, *i.e.*, Meta-World (Yu et al., 2019), RoboDesk (Kannan et al., 2021), and DeepMind Control Suite (DMC) (Tassa et al., 2018), including both cross-task and cross-environment setups (Meta-World → RoboDesk). Inspired by D4RL (Fu et al., 2020), we build offline datasets of *medium-replay* quality using DreamerV2 (Hafner et al., 2021). The datasets comprise all the samples in the replay buffer collected during the training process until the policy attains medium-level performance, defined as achieving 1/3 of the maximum score that the DreamerV2 agent can

achieve. Please refer to Appendix B.2 for further results of CoWorld trained with *medium-expert* offline data.

**Compared methods.** We compare CoWorld with both model-based and model-free RL approaches, including *Offline DV2* (Lu et al., 2023), *DrQ+BC* (Lu et al., 2023), *CQL* (Lu et al., 2023), *CURL* (Laskin et al., 2020), and *LOMPO* (Rafailov et al., 2021). In addition, we introduce the *DV2 Finetune* method, which involves taking a DreamerV2 (Hafner et al., 2021) model pretrained in the online source domain and subsequently finetuning it in the offline target dataset. Furthermore, *DV2 Finetune* can be integrated with the continual learning method, Elastic Weight Consolidation (EWC) (Kirkpatrick et al., 2017), to regularize the model for preserving source domain knowledge, *i.e.*, *Finetune+EWC*. Please refer to Appendix D for more details.

### 4.2. Cross-Task Experiments on Meta-World

**Setup.** Meta-World is an open-source simulated benchmark designed for solving a wide range of robot manipulation tasks. We select 6 tasks to serve as either the offline dataset or potential candidates for the online auxiliary domain. These tasks include: *Door Close (DC\*)*, *Button Press (BP)*, *Window Close (WC)*, *Handle Press (HP)*, *Drawer Close (DC)*, *Button Topdown (BT)*.

**Comparisons with offline visual RL methods.** As shown in Table 2, we compare the results of CoWorld with other models on Meta-World. CoWorld achieves the best performance in all 6 tasks. Notably, it outperforms *Offline DV2* (Lu et al., 2023), a method also built upon DreamerV2 and specifically designed for offline visual RL.

**Comparisons with online-to-offline finetuning.** In Table 2, *DV2 Finetune* achieves the second-best results by leveraging transferred knowledge from the auxiliary source domain. However, we observe that its performance experiences a notable decline in scenarios (*e.g.*, Meta-World → RoboDesk) involving significant data distribution shifts between the source and the target domains in visual observation, physical dynamics, reward definition, or even

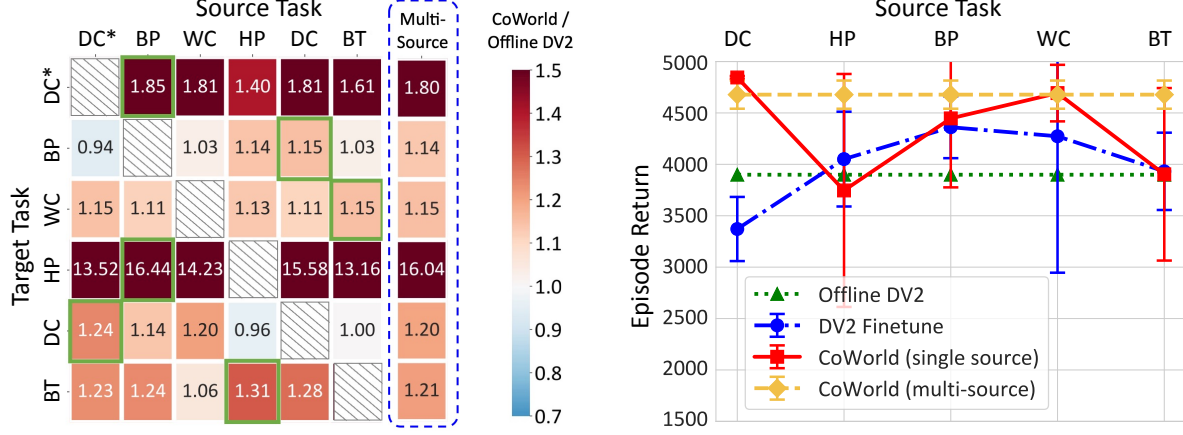


Figure 3. **Left:** The value in each grid signifies the ratios of returns achieved by CoWorld compared to *Offline DV2*. Highlighted grids represent the top-performing source domain. **Right:** Target returns on *Drawer Close* (DC\*) with different source domains. Multi-source CoWorld adaptively selects a useful source (*Door Close*) and achieves comparable results with the top-performing single-source CoWorld.

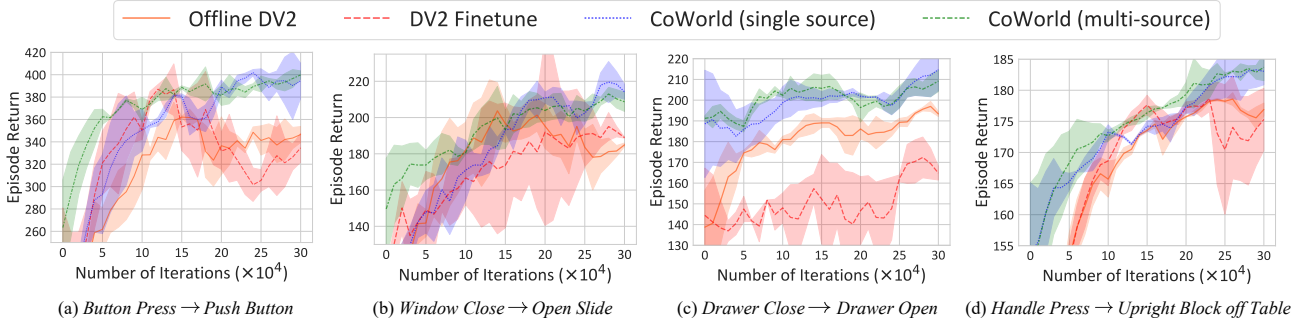


Figure 4. Quantitative results in domain transfer scenarios of Meta-World → RoboDesk.

the action space of the robots. Another important baseline model is *DV2 Finetune+EWG*, which focuses on mitigating the catastrophic forgetting of the knowledge obtained in source domain pretraining. Nevertheless, without additional model designs for domain adaptation, retaining source domain knowledge may eventually lead to a decrease in performance in the target domain. Moreover, it is interesting to observe that the LOMPO model suffers from the *negative transfer* effect when incorporating a source pretraining stage. It achieves an average return of 1,712 when it is trained from scratch in the offline domain while achieving an average return of 792 for online-to-offline finetuning. It implies that a naïve transfer learning method may degenerate the target performance by introducing unexpected bias.

**Results with a random source domain.** One may cast doubt on the influence of domain discrepancies between the auxiliary environment and the target offline dataset. In Figure 3 (Left), the transfer matrix of CoWorld among the 6 tasks of Meta-World is presented, where values greater than 1 indicate positive domain transfer effects. Notably, there are challenging cases with weakly related source and target tasks. In the majority of cases (26 out of 30), CoWorld outperforms *Offline DV2*, as illustrated in the heatmap.

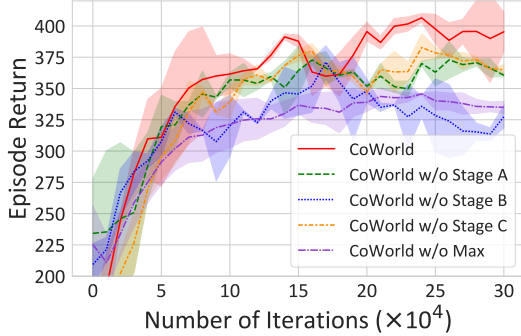
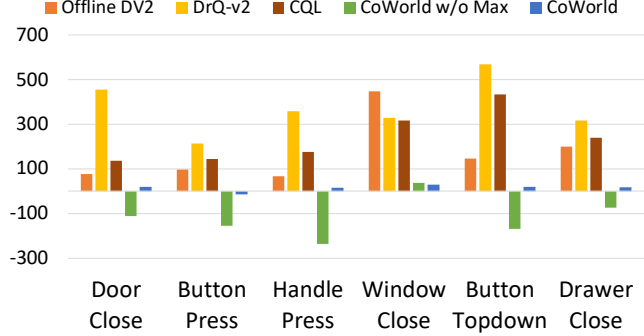
**Results with multiple source domains.** It is crucial to note that CoWorld can be easily extended to scenarios with multiple source domains by adaptively selecting a useful task as the auxiliary domain. From Table 2, we can see that the multi-source CoWorld achieves comparable results to the models trained with manually designated online simulators. In Figure 3 (Left), multi-source CoWorld achieves positive improvements over *Offline DV2* in all cases, approaching the best results of models using each source task as the auxiliary domain. In Figure 3 (Right), it also consistently outperforms the *DV2 Finetune* baseline model. These results demonstrate our approach’s ability to execute without strict assumptions about domain similarity and its ability to automatically identify a useful online simulator from a set of both related and less related source domains.

#### 4.3. Cross-Environments: Meta-World to RoboDesk

**Setup.** To explore cross-environment domain transfer, we employ four tasks from RoboDesk to construct individual offline datasets, as specified in Figure 4. These tasks require handling randomly positioned objects with image inputs. Table 1 presents the distinctions between the two environments in physical dynamics, action space, reward definitions, and

Table 3. Mean rewards and standard deviations of 10 episodes in offline DMC over 3 seeds.

MODEL	WW → WD	WW → WU	WW → WN	CR → CD	CR → CU	CR → CN	AVG.
OFFLINE DV2	435±22	139±4	214±4	243±7	3±1	51±4	181
DRQ+BC	291±10	299±15	318±40	663±15	202±12	132±33	355
CQL	46±19	64±32	29±2	2±1	52±57	111±157	51
CURL	43±5	21±3	23±3	26±7	4±2	11±4	21
LOMPO	462±87	260±21	<b>460±9</b>	395±52	46±19	120±4	291
DV2 FINETUNE	379±23	354±29	407±37	702±41	208±22	454±82	417
LOMPO FINETUNE	209±21	141±27	212±9	142±29	17±11	105±12	137
CoWORLD	<b>629±9</b>	<b>407±141</b>	426±32	<b>745±28</b>	<b>225±20</b>	<b>493±10</b>	<b>488</b>


 (a) Meta-World → RoboDesk (*Push Green Button*)


(b) Y-axis = Estimated value – True value

 Figure 5. (a) Ablation studies on **state alignment**, **reward alignment**, and **min-max value constraint**. (b) The disparities between the estimated value by various models and the true value. Please see the text in Section 4.5 for the implementation of *CoWorld w/o Max*.

visual appearances. For the best-source experiments, we manually select one source domain from Meta-World. For the multi-source experiments, we jointly use all aforementioned Meta-World tasks as the source domains.

**Results.** Figure 4 presents quantitative results of CoWorld, where it outperforms *Offline DV2* and *DV2 Finetune* by large margins. In contrast to prior findings, directly finetuning the source world model in this cross-environment setup, where there are more pronounced domain discrepancies, does not result in significant improvements in the final performance. In comparison, CoWorld more successfully addresses these challenges by leveraging domain-specific world models and RL agents, and explicitly aligning the state and reward spaces across domains. We also showcase the performance of multi-source CoWorld, which achieves comparable results to the *best-source* model that exclusively uses our designated source domain.

#### 4.4. Cross-Dynamics Experiments on DMC

**Setup.** DMC is a widely explored benchmark for continuous control. We use the *Walker* and *Cheetah* as the base agents and make modifications to the environment to create a set of 8 distinct tasks, i.e., *Walker Walk (WW)*, *Walker Downhill (WD)*, *Walker Uphill (WU)*, *Walker Nofoot (WN)*, *Cheetah Run (CR)*, *Cheetah Downhill (CD)*, *Cheetah Uphill (CU)*, *Cheetah Nopaw (CN)*. Particularly, *Walker Nofoot* is a task in which we cannot control the right foot of the

*Walker* agent. *Cheetah Nopaw* is a task in which we cannot control the front paw of the *Cheetah* agent.

**Results.** We apply the proposed multi-source domain selection method to build the domain transfer settings shown in Table 3. It is worth noting that CoWorld outperforms the other compared models in 5 out of 6 DMC offline datasets, and achieves the second-best performance in the remaining task. On average, it outperforms *Offline DV2* by 169.6% and outperforms *DrQ+BC* by 37.5%. Corresponding qualitative comparisons can be found in Appendix B.1.

#### 4.5. Further Analyses

**Ablation studies.** We conduct a series of ablation studies to validate the effectiveness of state space alignment (Stage A), reward alignment (Stage B), and min-max value constraint (Stage C). We show corresponding results on the offline *Push Green Button* dataset from RoboDesk in Figure 5(a). The performance experiences a significant decline when we abandon each training stage in CoWorld.

**Can CoWorld address value overestimation?** We evaluate the values estimated by the critic network of CoWorld on the offline Meta-World datasets when the training process is finished. In Figure 5(b), we compute the cumulative value predictions throughout 500 steps. The *true value* is determined by calculating the discounted sum of the actual rewards obtained by the actor in the same 500-steps period. We observe that existing approaches, including

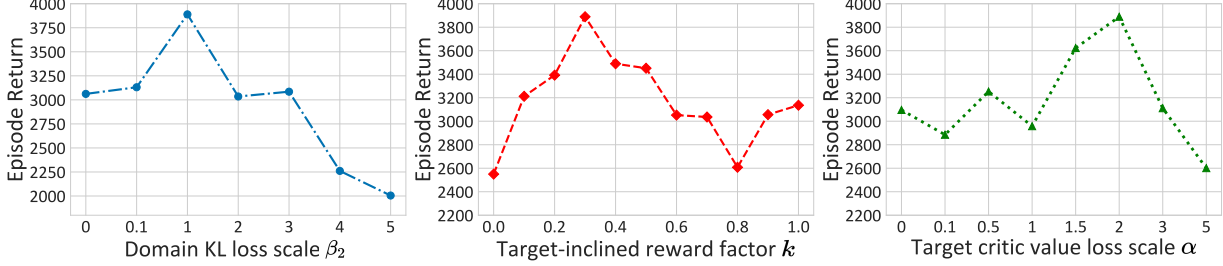


Figure 6. Sensitivity analysis of the hyperparameters on Meta-World ( $DC \rightarrow BP$ ).

*Offline DV2* and *CQL*, often overestimate the value functions in the offline setup. The baseline model “*CoWorld w/o Max*” is a variant of *CoWorld* that incorporates a brute-force constraint on the critic loss. It reformulates Eq. (6) as  $\sum_{t=1}^{H-1} \frac{1}{2} (v_\xi(\hat{z}_t) - \text{sg}(V_t))^2 + \alpha v_\xi(\hat{z}_t)$ . As observed, this model tends to underestimate the true value function, which can potentially result in overly conservative policies as a consequence. In contrast, the values estimated by *CoWorld* are notably more accurate and more akin to the true values.

**Hyperparameter sensitivity.** We conduct sensitivity analyses on Meta-World ( $DC \rightarrow BP$ ). From Figure 6, we observe that when  $\beta_2$  for the domain KL loss is too small, the state alignment between the source and target encoders becomes insufficient, hampering the transfer learning process. Conversely, if  $\beta_2$  is too large, the target encoder becomes excessively influenced by the source encoder, resulting in a decline in performance. We also find that the target-informed reward factor  $k$  plays a crucial role in balancing the influence of source data and target reward information, which achieves a consistent improvement over *DV2 Finetune* ( $2456 \pm 661$ ) in the range of  $[0.1, 0.7]$ . Moreover, we discover that the hyperparameter  $\alpha$  for the target value constraint performs well within  $[1, 3]$ , while an excessively larger  $\alpha$  may result in value over-conservatism in the target critic.

## 5. Related Work

**Offline visual RL.** Learning control policies from images is critical in real-world applications. Existing approaches can be grouped by the use of model-free (Laskin et al., 2020; Schwarzer et al., 2021; Stooke et al., 2021; Xiao et al., 2022; Parisi et al., 2022) or model-based (Hafner et al., 2019; 2020; 2021; Seo et al., 2022; Pan et al., 2022; Hafner et al., 2022; Mazzaglia et al., 2023; Micheli et al., 2023; Zhang et al., 2023; Ying et al., 2023) RL algorithms. In offline RL, agents leverage pre-collected offline data to optimize policies and encounter challenges associated with value overestimation (Levine et al., 2020). Previous methods mainly suggest taking actions that were previously present in the offline dataset or learning conservative value estimations (Fujimoto et al., 2019; Kumar et al., 2020; Chen et al., 2022; Yu et al., 2020; 2021; Rigter et al., 2022). Recent approaches have introduced specific techniques to address

the challenges associated with offline visual RL (Mandlekar et al., 2019; Dasari et al., 2019; Levine et al., 2020; Agarwal et al., 2020; Rafailov et al., 2021; Yu et al., 2022; Seo et al., 2022; Zang et al., 2023; Cho et al., 2022; Lu et al., 2023). Rafailov et al. (2021) proposed to handle high-dimensional observations with latent dynamics models and uncertainty quantification. Cho et al. (2022) proposed synthesizing the raw observation data to append the training buffer, aiming to mitigate the issue of overfitting. In a related study, Lu et al. (2023) established a competitive offline visual RL model based on DreamerV2 (Hafner et al., 2021), so that we use it as a significant baseline of our approach. In contrast to previous methods, we innovatively frame offline visual RL as an offline-online-offline transfer learning problem to allow for the use of auxiliary simulators to further mitigate the value overestimation issues.

**Transfer RL.** Our work is also related to transfer RL, which is known as to utilize the knowledge learned in past tasks to facilitate learning in unseen tasks (Zhu et al., 2020; Sekar et al., 2020; Zhang et al., 2020; Sun et al., 2021; Zhang et al., 2021; Eysenbach et al., 2021; Yang & Nachum, 2021; Sun et al., 2022; Ghosh et al., 2023; Kumar et al., 2023; Rafailov et al., 2023; Liu et al., 2023; Nakamoto et al., 2023). In the context intersected with visual RL, CtrlFormer (Mu et al., 2022) learns a transferable state representation via a sample-efficient vision Transformer. APV (Seo et al., 2022) executes action-free world model pretraining on source-domain videos and finetunes the model on downstream tasks. Choreographer (Mazzaglia et al., 2023) builds a model-based agent that exploits its world model to learn and adapt skills in imaginations, the learned skills are adapted to new domains using a meta-controller. VIP (Ma et al., 2023) presents a self-supervised, goal-conditioned value-function objective, which enables the use of unlabeled video data for model pretraining. Different from the aforementioned approaches, our study concentrates on performance within the offline domain, in the sense that we provide a pilot exploration of transfer learning for offline visual control.

## 6. Conclusions and Limitations

In this paper, we proposed a transfer RL method named *CoWorld*, which mainly tackles the difficulty in representa-



tion learning and value estimation in offline visual RL. The key idea is to exploit accessible online environments to train an auxiliary RL agent to offer additional value assessment. To address the domain discrepancies and to improve the offline policy, we present specific technical contributions of cross-domain *state alignment*, *reward alignment*, and *min-max value constraint*. CoWorld demonstrates competitive results across three RL benchmarks.

An unsolved problem of CoWorld is the increased computational complexity associated with the training phase in auxiliary domains (see Appendix B.5). It is valuable to improve the training efficiency in future research.

## 7. Broader Impacts

CoWorld is a transfer learning method that may benefit future research in the field of offline RL, model-based RL, and visual RL. Beyond the realm of reinforcement learning, this approach holds great potential to contribute to various domains such as robotics and autonomous driving.

A potential negative social impact of our method is the introduction of existing biases from the additional domain. If the training data used to develop our algorithm contains biases, the model may learn those biases, leading to unfair outcomes in decision-making processes. It’s crucial to carefully address biases in both data and algorithmic design to mitigate these negative social impacts.

## Acknowledgements

This work was supported by NSFC (62250062, U19B2035, 62106144), Shanghai Municipal Science and Technology Major Project (2021SHZDZX0102), the Fundamental Research Funds for the Central Universities, and Shanghai Sailing Program (21Z510202133) from the Science and Technology Commission of Shanghai Municipality.

## References

- Agarwal, R., Schuurmans, D., and Norouzi, M. An optimistic perspective on offline reinforcement learning. In *ICML*, pp. 104–114, 2020.
- Chen, H., Lu, C., Ying, C., Su, H., and Zhu, J. Offline reinforcement learning via high-fidelity generative behavior modeling. In *ICLR*, 2023.
- Chen, X., Ghadirzadeh, A., Yu, T., Wang, J., Gao, A. Y., Li, W., Bin, L., Finn, C., and Zhang, C. Lapo: Latent-variable advantage-weighted policy optimization for offline reinforcement learning. In *NeurIPS*, volume 35, pp. 36902–36913, 2022.
- Cho, D., Shim, D., and Kim, H. J. S2p: State-conditioned image synthesis for data augmentation in offline reinforcement learning. In *NeurIPS*, 2022.
- Clevert, D.-A., Unterthiner, T., and Hochreiter, S. Fast and accurate deep network learning by exponential linear units (elus). *arXiv preprint arXiv:1511.07289*, 2015.
- Dasari, S., Ebert, F., Tian, S., Nair, S., Bucher, B., Schmeckpeper, K., Singh, S., Levine, S., and Finn, C. Robonet: Large-scale multi-robot learning. In *CoRL*, 2019.
- Eysenbach, B., Asawa, S., Chaudhari, S., Levine, S., and Salakhutdinov, R. Off-dynamics reinforcement learning: Training for transfer with domain classifiers. In *ICLR*, 2021.
- Fu, J., Kumar, A., Nachum, O., Tucker, G., and Levine, S. D4rl: Datasets for deep data-driven reinforcement learning. *arXiv preprint arXiv:2004.07219*, 2020.
- Fujimoto, S. and Gu, S. S. A minimalist approach to offline reinforcement learning. In *NeurIPS*, 2021.
- Fujimoto, S., Meger, D., and Precup, D. Off-policy deep reinforcement learning without exploration. In *ICML*, pp. 2052–2062, 2019.
- Ghosh, D., Bhateja, C., and Levine, S. Reinforcement learning from passive data via latent intentions. *arXiv preprint arXiv:2304.04782*, 2023.
- Hafner, D., Lillicrap, T., Fischer, I., Villegas, R., Ha, D., Lee, H., and Davidson, J. Learning latent dynamics for planning from pixels. In *ICML*, pp. 2555–2565, 2019.
- Hafner, D., Lillicrap, T., Ba, J., and Norouzi, M. Dream to control: Learning behaviors by latent imagination. In *ICLR*, 2020.
- Hafner, D., Lillicrap, T., Norouzi, M., and Ba, J. Mastering atari with discrete world models. In *ICLR*, 2021.
- Hafner, D., Lee, K.-H., Fischer, I., and Abbeel, P. Deep hierarchical planning from pixels. *arXiv preprint arXiv:2206.04114*, 2022.
- Kannan, H., Hafner, D., Finn, C., and Erhan, D. Robodesk: A multi-task reinforcement learning benchmark. <https://github.com/google-research/robodesk>, 2021.
- Kirkpatrick, J., Pascanu, R., Rabinowitz, N., Veness, J., Desjardins, G., Rusu, A. A., Milan, K., Quan, J., Ramalho, T., Grabska-Barwinska, A., et al. Overcoming catastrophic forgetting in neural networks. *Proceedings of the national academy of sciences*, 114(13):3521–3526, 2017.
- Kumar, A., Zhou, A., Tucker, G., and Levine, S. Conservative q-learning for offline reinforcement learning. In *NeurIPS*, volume 33, pp. 1179–1191, 2020.

- Kumar, A., Agarwal, R., Geng, X., Tucker, G., and Levine, S. Offline q-learning on diverse multi-task data both scales and generalizes. In *ICLR*, 2023.
- Laskin, M., Srinivas, A., and Abbeel, P. Curl: Contrastive unsupervised representations for reinforcement learning. In *ICML*, pp. 5639–5650, 2020.
- Levine, S., Kumar, A., Tucker, G., and Fu, J. Offline reinforcement learning: Tutorial, review, and perspectives on open problems. *arXiv preprint arXiv:2005.01643*, 2020.
- Liu, X., Chen, Y., Li, H., Li, B., and Zhao, D. Cross-domain random pre-training with prototypes for reinforcement learning. *arXiv preprint arXiv:2302.05614*, 2023.
- Lu, C., Ball, P. J., Rudner, T. G., Parker-Holder, J., Osborne, M. A., and Teh, Y. W. Challenges and opportunities in offline reinforcement learning from visual observations. *Transactions on Machine Learning Research*, 2023.
- Ma, Y. J., Sodhani, S., Jayaraman, D., Bastani, O., Kumar, V., and Zhang, A. Vip: Towards universal visual reward and representation via value-implicit pre-training. In *ICLR*, 2023.
- Mandlekar, A., Booher, J., Spero, M., Tung, A., Gupta, A., Zhu, Y., Garg, A., Savarese, S., and Fei-Fei, L. Scaling robot supervision to hundreds of hours with roboturk: Robotic manipulation dataset through human reasoning and dexterity. In *IROS*, pp. 1048–1055, 2019.
- Mazzaglia, P., Verbelen, T., Dhoedt, B., Lacoste, A., and Rajeswar, S. Choreographer: Learning and adapting skills in imagination. In *ICLR*, 2023.
- Micheli, V., Alonso, E., and Fleuret, F. Transformers are sample efficient world models. In *ICLR*, 2023.
- Mu, Y. M., Chen, S., Ding, M., Chen, J., Chen, R., and Luo, P. Ctrlformer: Learning transferable state representation for visual control via transformer. In *ICML*, pp. 16043–16061, 2022.
- Nakamoto, M., Zhai, Y., Singh, A., Mark, M. S., Ma, Y., Finn, C., Kumar, A., and Levine, S. Cal-ql: Calibrated offline rl pre-training for efficient online fine-tuning. *arXiv preprint arXiv:2303.05479*, 2023.
- Pan, M., Zhu, X., Wang, Y., and Yang, X. Iso-dream: Isolating and leveraging noncontrollable visual dynamics in world models. In *NeurIPS*, volume 35, pp. 23178–23191, 2022.
- Parisi, S., Rajeswaran, A., Purushwalkam, S., and Gupta, A. The unsurprising effectiveness of pre-trained vision models for control. In *ICML*, pp. 17359–17371, 2022.
- Qi, H., Su, Y., Kumar, A., and Levine, S. Data-driven offline decision-making via invariant representation learning. In *NeurIPS*, 2022.
- Rafailov, R., Yu, T., Rajeswaran, A., and Finn, C. Offline reinforcement learning from images with latent space models. In *Proceedings of Machine Learning Research*, pp. 1154–1168, 2021.
- Rafailov, R., Hatch, K. B., Koley, V., Martin, J. D., Phielipp, M., and Finn, C. MOTO: Offline pre-training to online fine-tuning for model-based robot learning. In *7th Annual Conference on Robot Learning*, 2023. URL <https://openreview.net/forum?id=6Um8P8Fvyhl>.
- Rigter, M., Lacerda, B., and Hawes, N. Rambo-rl: Robust adversarial model-based offline reinforcement learning. In *NeurIPS*, 2022.
- Schwarzer, M., Rajkumar, N., Noukhovitch, M., Anand, A., Charlin, L., Hjelm, R. D., Bachman, P., and Courville, A. C. Pretraining representations for data-efficient reinforcement learning. In *NeurIPS*, volume 34, pp. 12686–12699, 2021.
- Sekar, R., Rybkin, O., Daniilidis, K., Abbeel, P., Hafner, D., and Pathak, D. Planning to explore via self-supervised world models. In *ICML*, pp. 8583–8592, 2020.
- Seo, Y., Lee, K., James, S. L., and Abbeel, P. Reinforcement learning with action-free pre-training from videos. In *ICML*, pp. 19561–19579, 2022.
- Stooke, A., Lee, K., Abbeel, P., and Laskin, M. Decoupling representation learning from reinforcement learning. In *ICML*, pp. 9870–9879, 2021.
- Sun, Y., Yin, X., and Huang, F. Temple: Learning template of transitions for sample efficient multi-task rl. In *AAAI*, volume 35, pp. 9765–9773, 2021.
- Sun, Y., Zheng, R., Wang, X., Cohen, A., and Huang, F. Transfer rl across observation feature spaces via model-based regularization. In *ICLR*, 2022.
- Tassa, Y., Doron, Y., Muldal, A., Erez, T., Li, Y., Casas, D. d. L., Budden, D., Abdolmaleki, A., Merel, J., Lefrancq, A., et al. Deepmind control suite. *arXiv preprint arXiv:1801.00690*, 2018.
- Xiao, T., Radosavovic, I., Darrell, T., and Malik, J. Masked visual pre-training for motor control. *arXiv preprint arXiv:2203.06173*, 2022.
- Yang, M. and Nachum, O. Representation matters: offline pretraining for sequential decision making. In *ICML*, pp. 11784–11794, 2021.

- Yarats, D., Fergus, R., Lazaric, A., and Pinto, L. Mastering visual continuous control: Improved data-augmented reinforcement learning. *arXiv preprint arXiv:2107.09645*, 2021.
- Ying, C., Hao, Z., Zhou, X., Su, H., Liu, S., Li, J., Yan, D., and Zhu, J. Reward informed dreamer for task generalization in reinforcement learning. *arXiv preprint arXiv:2303.05092*, 2023.
- Yu, T., Quillen, D., He, Z., Julian, R., Hausman, K., Finn, C., and Levine, S. Meta-world: A benchmark and evaluation for multi-task and meta reinforcement learning. In *CoRL*, 2019.
- Yu, T., Thomas, G., Yu, L., Ermon, S., Zou, J. Y., Levine, S., Finn, C., and Ma, T. Mopo: Model-based offline policy optimization. In *NeurIPS*, volume 33, pp. 14129–14142, 2020.
- Yu, T., Kumar, A., Rafailov, R., Rajeswaran, A., Levine, S., and Finn, C. Combo: Conservative offline model-based policy optimization. In *NeurIPS*, volume 34, pp. 28954–28967, 2021.
- Yu, T., Kumar, A., Chebotar, Y., Hausman, K., Finn, C., and Levine, S. How to leverage unlabeled data in offline reinforcement learning. In *ICML*, pp. 25611–25635, 2022.
- Zang, H., Li, X., Yu, J., Liu, C., Islam, R., Combes, R. T. D., and Larocche, R. Behavior prior representation learning for offline reinforcement learning. In *ICLR*, 2023.
- Zhang, A., Lyle, C., Sodhani, S., Filos, A., Kwiatkowska, M., Pineau, J., Gal, Y., and Precup, D. Invariant causal prediction for block mdps. In *ICML*, pp. 11214–11224, 2020.
- Zhang, A., McAllister, R., Calandra, R., Gal, Y., and Levine, S. Learning invariant representations for reinforcement learning without reconstruction. In *ICLR*, 2021.
- Zhang, W., Chen, G., Zhu, X., Gao, S., Wang, Y., and Yang, X. Predictive experience replay for continual visual control and forecasting. *arXiv preprint arXiv:2303.06572*, 2023.
- Zhu, Z., Lin, K., Jain, A. K., and Zhou, J. Transfer learning in deep reinforcement learning: A survey. *arXiv preprint arXiv:2009.07888*, 2020.
- Zhuang, Z., Lei, K., Liu, J., Wang, D., and Guo, Y. Behavior proximal policy optimization. In *ICLR*, 2023.

## A. Model Details

### A.1. Framework of CoWorld

As illustrated in Figure 7, the entire training process of CoWorld comprises three iterative stages: offline-to-online state alignment (Stage A), online-to-offline reward alignment (Stage B), and online-to-offline value constraint (Stage C). First, we feed the same target domain observations sampled from  $\mathcal{B}^{(T)}$  into the encoders and close the distance of  $e_{\phi'}(o_t^{(T)})$  and  $e_{\phi}(o_t^{(T)})$  in Stage A. Second, in Stage B, the source reward predictor  $r_{\phi'}(\cdot)$  is trained with mixed data from both of the replay buffers  $\mathcal{B}^{(S)}$  and  $\mathcal{B}^{(T)}$ . Notably, when we sample data from  $\mathcal{B}^{(T)}$ , the reward will be relabelled as the target-informed source reward. Finally, we introduce a min-max value constraint using the source critic to the target critic in Stage C.

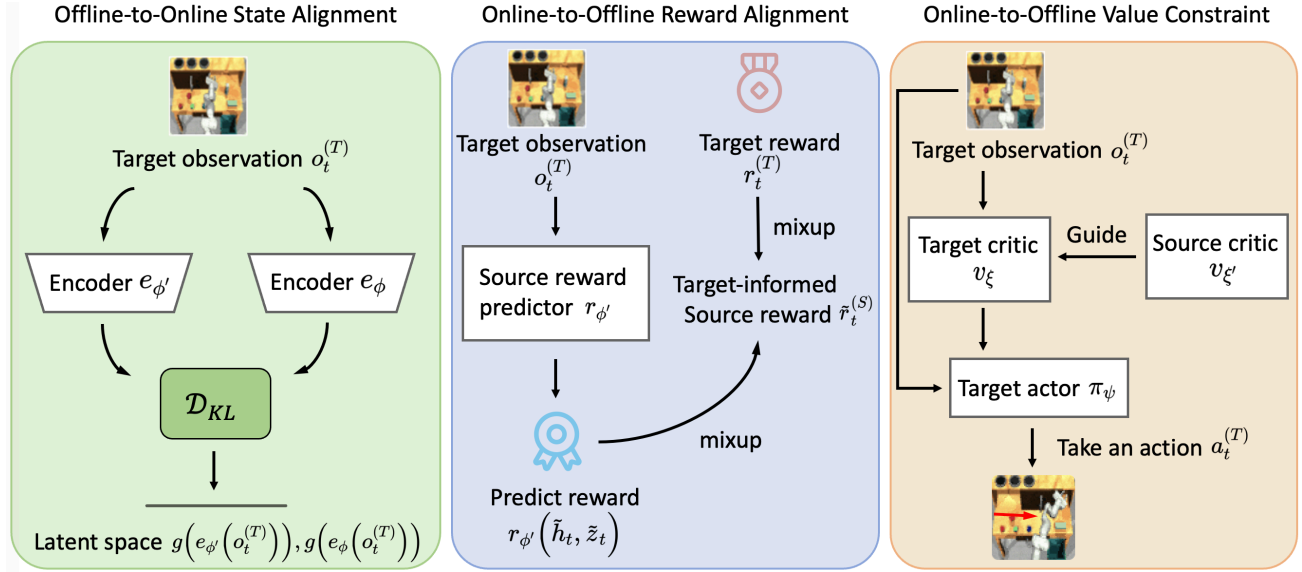


Figure 7. CoWorld uses an auxiliary online environment to build a policy “test bed” that is aware of offline domain information. This, in turn, can guide the visual RL agent in the offline domain to learn a mildly-conservative policy, striking a balance between value overestimation and over-conservatism.

### A.2. World Model Learning

We adopt the framework of the world model used in (Hafner et al., 2021). The image encoder is a Convolutional Neural Network (CNN). The image predictor is a transposed CNN and the transition, reward, and discount factor predictors are Multi-Layer Perceptrons (MLPs). The discount factor predictor serves as an estimate of the probability that an episode will conclude while learning behavior based on model predictions. The encoder and decoder take  $64 \times 64$  images as inputs.

The loss function of the target world model (*i.e.*, Eq. (3)) is jointly minimized with respect to the  $\phi'$  that contains all parameters of the target world model. The image predictor, reward predictor, discount predictor, and transition predictor are trained to maximize the log-likelihood of their individual targets through the distributions they produce.

### A.3. Behavior Learning

For behavior learning of CoWorld, we use the actor-critic learning architecture of DreamerV2 (Hafner et al., 2021). The  $\lambda$ -target  $V_t^{(T)}$  in Eq. (6) is defined as follows:

$$V_t^{(T)} \doteq \hat{r}_t^{(T)} + \hat{\gamma}_t^{(T)} \begin{cases} (1 - \lambda)v_{\xi}(\hat{z}_{t+1}^{(T)}) + \lambda V_{t+1}^{(T)} & \text{if } t < H \\ v_{\xi}(\hat{z}_H^{(T)}) & \text{if } t = H \end{cases}, \quad (8)$$

where  $\lambda$  is set to 0.95 for considering more on long horizon targets. The actor and critic are both MLPs with ELU (Clevert et al., 2015) activations while the world model is fixed. The target actor and critic are trained with guidance from the source critic, and regress the  $\lambda$ -return with a squared loss.



Table 4. Performance on DMC *medium-expert* dataset. We report the mean rewards and standard deviations of 10 episodes over 3 seeds.

MODEL	WW → WD	WW → WU	WW → WN	CR → CD	CR → CU	CR → CN	AVG.
OFFLINE DV2	450 ± 24	141 ± 1	214 ± 8	248 ± 9	3 ± 0	48 ± 3	184
DRQ+BC	808 ± 47	762 ± 61	808 ± 45	862 ± 13	454 ± 12	730 ± 17	737
LOMPO	548 ± 245	449 ± 117	688 ± 97	174 ± 29	19 ± 10	113 ± 35	332
FINETUNE	784 ± 46	671 ± 65	851 ± 91	858 ± 9	428 ± 49	833 ± 7	738
CoWORLD	<b>848 ± 9</b>	<b>774 ± 29</b>	<b>919 ± 7</b>	<b>871 ± 13</b>	<b>475 ± 16</b>	<b>844 ± 1</b>	<b>789</b>

The source actor and critic are:

$$\begin{aligned}
 \text{Source Actor:} \quad & \hat{a}_t^{(S)} \sim \pi_{\psi'}(\hat{a}_t^{(S)} | \hat{z}_t^{(S)}) \\
 \text{Source Critic:} \quad & v_{\xi'}(\hat{z}_t^{(S)}) \approx \mathbb{E}_{p_{\phi'}, p_{\psi'}} \left[ \sum_{\tau \geq t} \hat{\gamma}_{\tau-t}^{(S)} \hat{r}_{\tau}^{(S)} \right].
 \end{aligned} \tag{9}$$

We train the source actor  $\pi_{\psi'}$  by maximizing an objective function:

$$\mathcal{L}(\psi') = \mathbb{E}_{p_{\phi'}, p_{\psi'}} \left[ \underbrace{\sum_{t=1}^{H-1} (\beta H [a_t^{(S)} | \hat{z}_t^{(S)}])}_{\text{entropy regularization}} + \underbrace{\rho V_t^{(S)}}_{\text{dynamics backprop}} + \underbrace{(1 - \rho) \ln \pi_{\psi'}(\hat{a}_t^{(S)} | \hat{z}_t^{(S)}) \text{sg}(V_t^{(S)} - v_{\xi'}(\hat{z}_t^{(S)}))}_{\text{REINFORCE}} \right]. \tag{10}$$

The source critic  $v_{\xi'}$  is optimized by minimizing a loss function:

$$\mathcal{L}(\xi') = \mathbb{E}_{p_{\phi'}, p_{\psi'}} \left[ \sum_{t=1}^{H-1} \frac{1}{2} \left( v_{\xi'}(\hat{z}_t^{(S)}) - \text{sg}(V_t^{(S)}) \right)^2 \right]. \tag{11}$$

## B. Additional Quantitative and Qualitative Results

### B.1. Visualizations on Policy Evaluation

We evaluate the trained agent of different models on the Meta-World and DMC tasks and select the first 45 frames for comparison. Figure 8 and Figure 9 present showcases of performing the learned policies of different models on DMC and Meta-World respectively.

### B.2. Quantitative Results on DMC *Medium-Expert* Dataset

Similar to the data collection strategy of *medium-replay* dataset, we build offline datasets of *medium-expert* quality using a DreamerV2 agent.

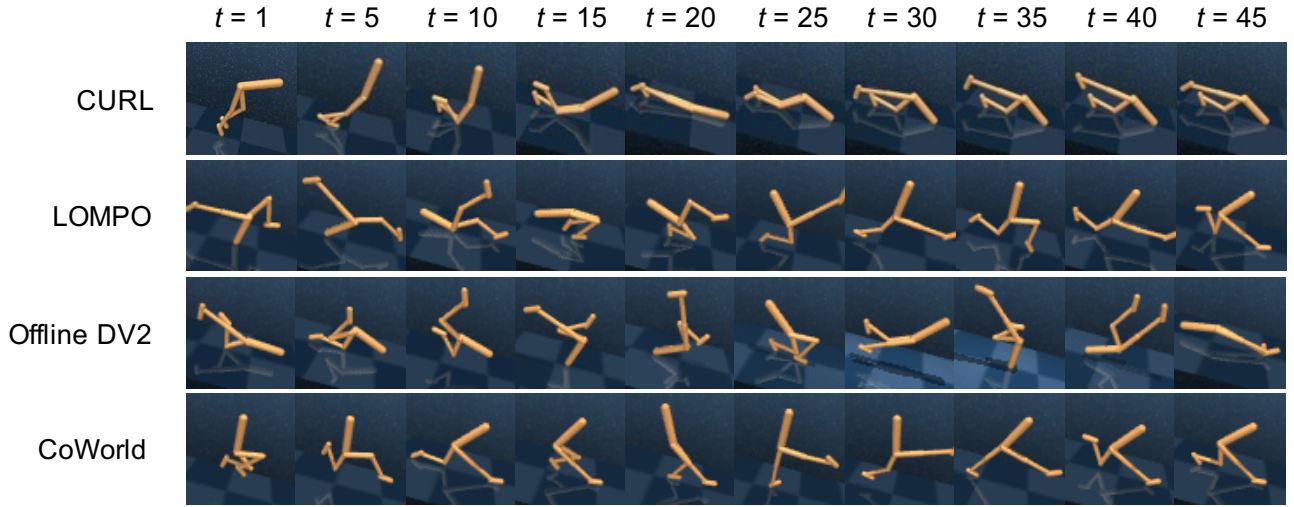
The *medium-expert* dataset comprises all the samples in the replay buffer during the training process until the policy attains expert-level performance, defined as achieving the maximum score that the DreamerV2 agent can achieve. As shown in Table 4, CoWorld outperforms other baselines on the DMC *medium-expert* dataset in most tasks.

### B.3. Quantitative Results on Meta-World

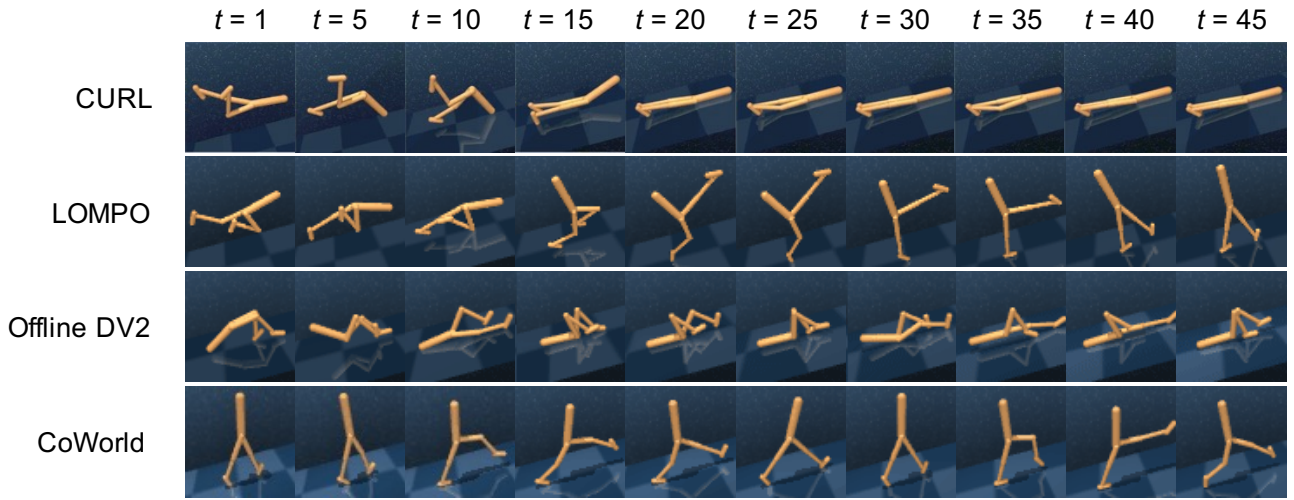
Figure 10(a) compares the performance of different models on Meta-World. *DV2 Finetune* demonstrates better performance in the initial training phase, thanks to its direct access to the source environment. Instead, CoWorld introduces auxiliary source value guidance to assist the training of the target agent. In the final phase of training, the source value guidance is more effective, and then CoWorld outperforms *DV2 Finetune*. Furthermore, Figure 10(b) presents the ablation studies of CoWorld conducted on Meta-World, highlighting the effectiveness and necessity of each training stage.

### B.4. Effect of Latent Space Alignment

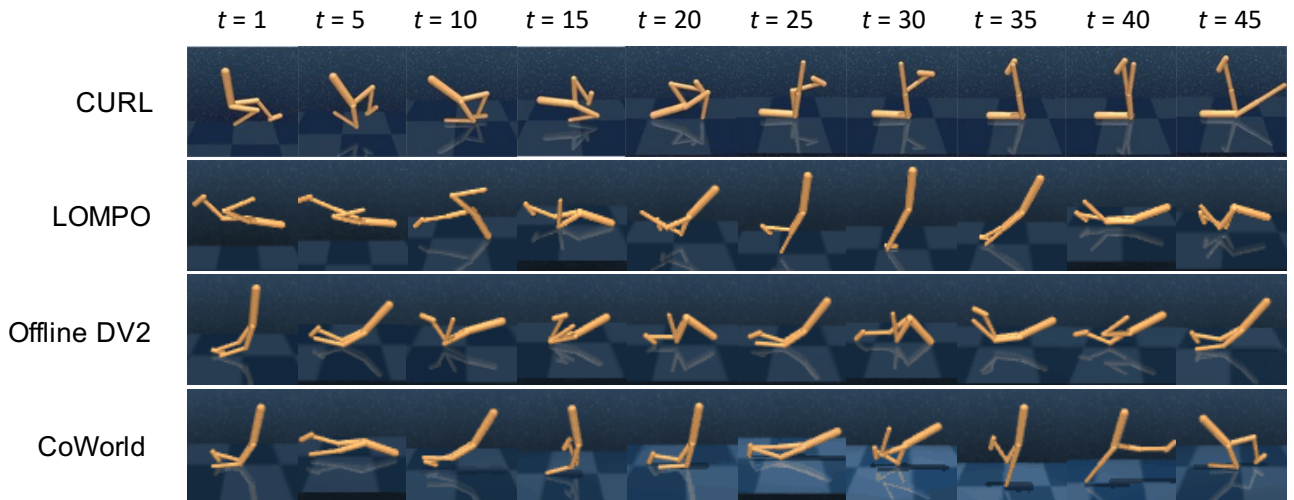
We feed the same observations into the source and target encoder of CoWorld and then use the t-distributed stochastic neighbor embedding (t-SNE) method to visualize the latent states. As shown in Figure 11, the representation learning alignment bridges the gap between the hidden state distributions of the source encoder and target encoder.



(a) Policy evaluation on the DMC Walker Downhill task



(b) Policy evaluation on the DMC Walker Uphill task



(c) Policy evaluation on the DMC Walker Nofoot task

Figure 8. Additional qualitative results of policy evaluation on the DMC tasks.

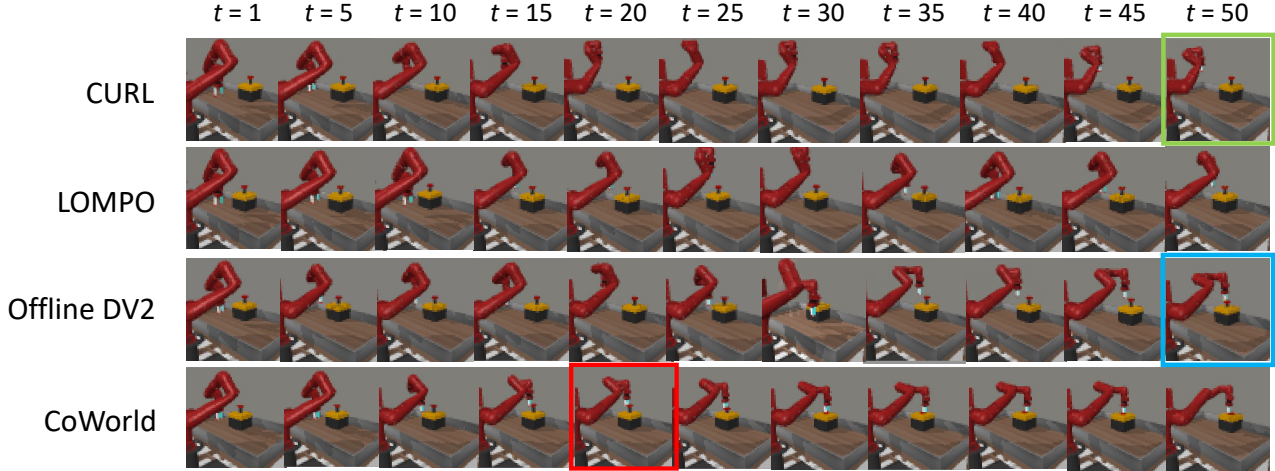


Figure 9. Policy evaluation on the Meta-World *Button Topdown* task. The performance of model-free method *CURL* is poor and it cannot complete the task (green box). CoWorld achieves better performance and completes the task in fewer steps (red box) than *Offline DV2* (blue box).

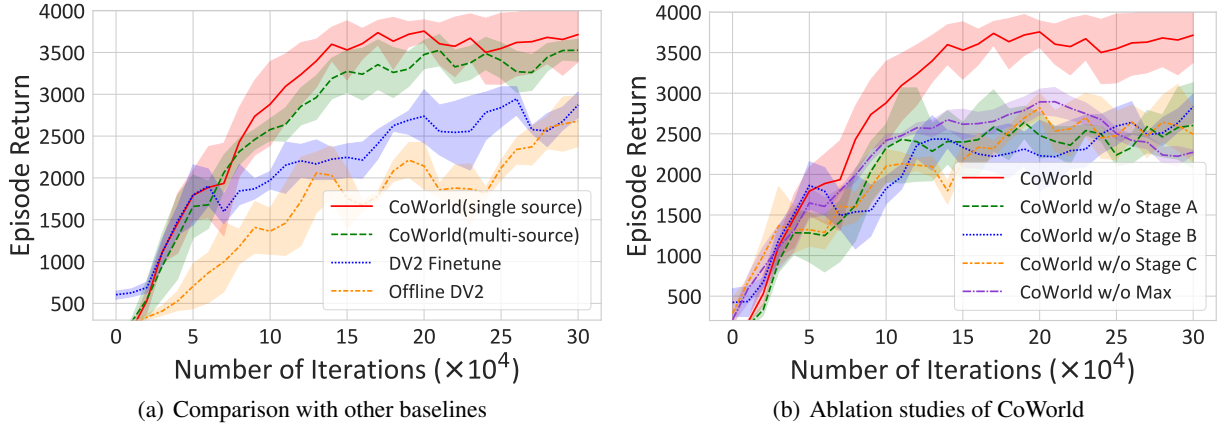


Figure 10. (a) Comparison with various approaches on the Meta-World *Button Press* task. (b) Ablation studies on the Meta-World *Button Press* task that can show the effect of state alignment (green), reward alignment (purple), and min-max value constraint (orange).

### B.5. Training Efficiency

As presented in Table 5, we evaluate the training/inference time on the Meta-World benchmark (Handle Press  $\rightarrow$  Button Topdown) using a single RTX 3090 GPU.

## C. Details of Multi-Source CoWorld

The key idea of adaptive domain selection of multi-source CoWorld is to allocate a set of one-hot weights  $\omega_t^{i=1:N}$  to candidate source domains by calculating their KL divergence in the latent state space to the target domain, where  $i \in [1, N]$  is the index of each source domain. The adaptive domain selection procedure includes the following steps:

1. **World models pretraining.** We pretrain a world model for each source domain and target domain individually.
2. **Domain distance measurement.** At each training step in the target domain, we measure the KL divergence between the latent states of the target domain, produced by  $e_\phi(o_t^{(T)})$ , and corresponding states in each source domain, produced by  $e_{\phi'_i}(o_t^{(T)})$ . Here,  $e_\phi^{(T)}$  is the encoder of the target world model and  $e_{\phi'_i}$  is the encoder of the world model for the source domain  $i$ .
3. **Auxiliary domain identification.** We dynamically identify the closest source domain with the smallest KL divergence. We set  $\omega_t^{i=1:N}$  as a one-hot vector, where  $\omega_t^i = 1$  indicates the selected auxiliary domain.

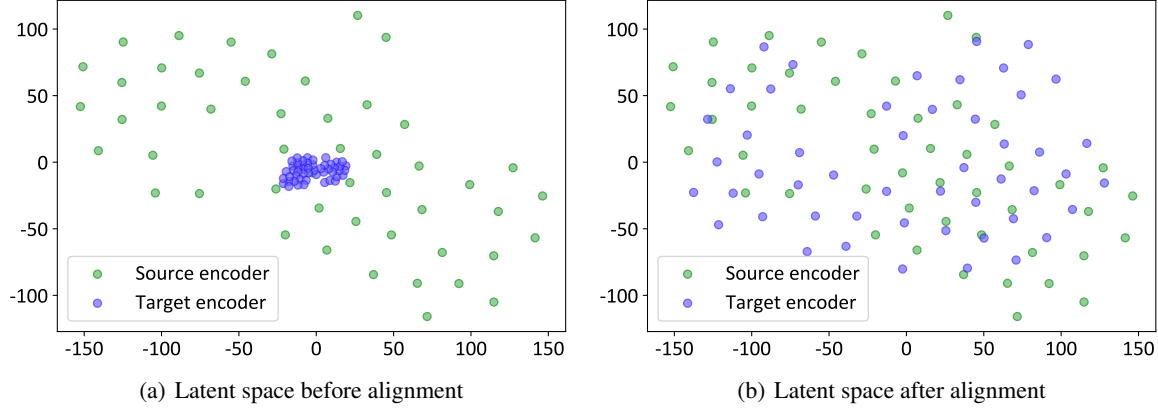


Figure 11. Visualization of the latent space alignment on Meta-World *Handle Press*  $\rightarrow$  *Button Press* task by the t-SNE method. (a) Latent space of CoWorld before alignment. (b) Latent space of CoWorld after alignment.

Table 5. Time complexity on the Meta-World HP  $\rightarrow$  BT task.

Model	Number of Training Iterations	Training Time	Inference Time Per Episode
Offline DV2	300k	2054 min	2.95 sec
DrQ+BC	300k	200 min	2.28 sec
CQL	300k	405 min	1.88 sec
CURL	300k	434 min	2.99 sec
LOMPO	100k	1626 min	4.98 sec
DV2 Finetune	460k	1933 min	6.63 sec
DV2 Finetune+EWC	460k	1533 min	5.58 sec
CoWorld	460k	3346 min	4.47 sec

4. **Rest of training.** With the one-hot weights, we continue the rest of the proposed online-to-offline training approach. For example, during representation learning, we adaptively align the target state space to the selected online simulator by rewriting the domain alignment loss term in Eq. (3) as

$$\mathcal{L}_{M-S} = \beta_2 \sum_{i=1}^N \omega_i \text{KL} \left[ \text{sg}(g(e_{\phi'}(o_i^{(T)}))) \parallel g(e_{\phi}(o_i^{(T)})) \right]. \quad (12)$$

To evaluate the effectiveness of the multi-source adaptive selection algorithm, we conducted experiments on Meta-World and RoboDesk Benchmark. For each target task, two source tasks are utilized, including the CoWorld best-performing task and the CoWorld worst-performing task. Additionally, the sub-optimal source task is added for some target tasks.

As shown in Table 6, multi-source CoWorld can adaptively select the best source task for most multi-source problems to ensure adequate knowledge transfer. The performance of multi-source CoWorld is reported in Table 2. CoWorld can flexibly adapt to the transfer learning scenarios with multiple source domains, achieving comparable results to the model that exclusively uses our manually designated auxiliary simulator as the source domain (best source). This study significantly improves the applicability of CoWorld in broader scenarios.

## D. Compared Methods

We compare CoWorld with several widely used model-based and model-free offline methods.

- **Offline DV2** (Lu et al., 2023): A model-based RL method that modifies DreamerV2 (Hafner et al., 2021) to offline setting, and adds a reward penalty corresponding to the mean disagreement of the dynamics ensemble.
- **DrQ+BC** (Lu et al., 2023): It modifies the policy loss term in DrQ-v2 (Yarats et al., 2021) to match the loss given in (Fujimoto & Gu, 2021).
- **CQL** (Lu et al., 2023): It is a framework for offline RL that learns a Q-function that guarantees a lower bound for the



Table 6. Multi-source CoWorld selection results on Meta-World and RoboDesk.

Target Task	Selected Source Task
Door Close	Drawer Close
Button Press	Handle Press
Window Close	Button Topdown
Handle Press	Button Press
Button Topdown	Handle Press
Drawer Close	Door Close
RoboDesk Push Button	Button Press
RoboDesk Open Slide	Window Close
RoboDesk Drawer Open	Drawer Close
RoboDesk Upright Block off Table	Handle Press

expected policy value than the actual policy value. We add the CQL regularizers to the Q-function update of DrQ-v2 (Kumar et al., 2020).

- **CURL** (Laskin et al., 2020): It is a model-free RL approach that extracts high-level features from raw pixels utilizing contrastive learning.
- **LOMPO** (Rafailov et al., 2021): An offline model-based RL algorithm that handles high-dimensional observations with latent dynamics models and uncertainty quantification.
- **LOMPO Finetune** (Rafailov et al., 2021): It pretrains a LOMPO agent with source domain data and subsequently finetunes the pretrained agent in the offline target domain.
- **DV2 Finetune**: It pretrains a DreamerV2 agent in the online source domain and subsequently finetunes the pretrained agent in the offline target domain. Notably, Meta-World  $\rightarrow$  RoboDesk tasks’ action space is inconsistent, and we can’t finetune directly. Instead, we use the maximum action space of both environments as the shared policy output dimension. For Meta-World and Meta-World  $\rightarrow$  RoboDesk transfer tasks, pretrain the agent 160k steps, and finetune it 300k steps. For DMC transfer tasks, pretrain the agent 600k steps, and finetune it 600k steps.
- **DV2 Finetune+EWC**: It modifies the *DV2 Finetune* method with EWC to regularize the model for retaining knowledge from the online source domain. The steps of pretraining and finetuning are consistent with *DV2 Finetune*.

## E. Implementation Details

**Meta-World.** For the Meta-World environment, we adopt robotic control tasks with complex visual dynamics. For instance, the *Door Close* task requires the agent to close a door with a revolving joint while randomizing the door positions, and the *Handle Press* task involves pressing a handle down while randomizing the handle positions. To evaluate the performance of CoWorld on these tasks, we compare it with several baselines in six visual RL transfer tasks.

**RoboDesk.** In our study, we select Meta-World as the source domain and RoboDesk as the target domain. Notably, there exists a significant domain gap between these two environments. The visual observations, physical dynamics and action spaces of two environments are different. First, Meta-World adopts a side viewpoint, while RoboDesk utilizes a top viewpoint. Further, the action space of Meta-World is 4 dimensional, while RoboDesk comprises a 5-dimensional action space. Considering these differences, the Meta-World  $\rightarrow$  RoboDesk presents a challenging task for transfer learning.

**DeepMind Control.** Source agents are trained with standard DMC environments, target agents are trained in modified DMC environments. In this modified environment, *Walker Uphill* and *Cheetah Uphill* represent the task in which the plane is a  $15^\circ$  uphill slope. *Walker Downhill* and *Cheetah Downhill* represents the task in which the plane is a  $15^\circ$  downhill slope. We evaluate our model with baselines in six tasks with different source domains and target domains.

## F. Assumptions of the Similarity between the Source and Target Domains

We assume that there exist notable distinctions between the source and target domains (see Table 1). This assumption can be softened by our proposed approaches of state and reward alignment. Through these approaches, we aim to mitigate domain discrepancies between distinct source and target MDPs. Empirical evidence supporting our methods is presented in Section 4.3, where our proposed approach demonstrates robust performance in the Meta-World  $\rightarrow$  RoboDesk transfer RL setup.

Our experiments reveal that the CoWorld method exhibits a notable tolerance to inter-domain differences in visual observation, physical dynamics, reward definition, or even the action space of the robots. This characteristic makes it more convenient to choose an auxiliary simulator based on the type of robot. For example:

- When the target domain involves a robotic arm (*e.g.*, RoboDesk), an existing robotic arm simulation environment (*e.g.*, Meta-World as used in our paper) can be leveraged as the source domain.
- In scenarios with legged robots, environments like DeepMind Control with Humanoid tasks can serve as suitable auxiliary simulators.
- For target domains related to autonomous driving vehicles, simulation environments like CARLA can be selected.

## G. Hyperparameters

The hyperparameters of CoWorld are shown in Table 7.

Table 7. Hyperparameters of CoWorld.

Name	Notation	Value	
Co-training		Meta-World/RoboDesk	DMC
Domain KL loss scale	$\beta_2$	1	1.5
Target-informed reward factor	$k$	0.3	0.9
Target critic value loss scale	$\alpha$	2	1
Source domain update iterations	$K_1$	$2 \cdot 10^4$	$2 \cdot 10^4$
Target domain update iterations	$K_2$	$5 \cdot 10^4$	$2 \cdot 10^4$
World Model			
Dataset size	—	$2 \cdot 10^6$	
Batch size	$B$	50	
Sequence length	$L$	50	
KL loss scale	$\beta_1$	1	
Discrete latent dimensions	—	32	
Discrete latent classes	—	32	
RSSM number of units	—	600	
World model learning rate	—	$2 \cdot 10^{-4}$	
Behavior Learning			
Imagination horizon	$H$	15	
Discount	$\gamma$	0.995	
$\lambda$ -target	$\lambda$	0.95	
Actor learning rate	—	$4 \cdot 10^{-5}$	
Critic learning rate	—	$1 \cdot 10^{-4}$	